

Effect of surface treatment by sandblasting on the quality and electrochemical corrosion properties of a C-1020 carbon steel used by an Algerian oil company

Nadia HAMMOUDA*, and Kamel BELMOKRE

Department of chemistry, Faculty of Sciences, 20 Août 1955 university-Route d'El Hadaiek, B.P 26, Skikda-Algeria

Abstract. The purpose of the different operations under the term surface preparation is to get a clean surface able to be coated. It is essential to adapt this preparation in terms of the metallurgical nature of the substrate, cleanliness, its shape and roughness. Surface preparations especially the operations of sandblasting, polishing, or grinding prove of capital importance. It allows to modify the superficial properties of these materials, after these treatments the surface becomes very active. This paper evaluates the mechanical surface treatments effect by sandblasting (Sa 1.5 and Sa 2.5) on the electrochemical corrosion characteristics of C-1020 carbon steel in 3% NaCl solution electrolyte simulating aggressive sea atmosphere. Investigations are conducted using stationary (free potential "E-t, polarization curves "E-i", the Tafel rights and the Rp) and non-stationary electrochemical tools such as electrochemical impedance. The results obtained allowed us to highlight that sandblasted carbon steel degrades with immersion time because of the roughness of the surface. These results were confirmed by the plot of the electrochemical impedance diagrams, confirming that the process governing kinetics is under charge transfer control. Good protection against corrosion cannot be obtained only with a good surface preparation of the adapted steel.

1 Introduction

Corrosion is a material degradation caused by the chemical reaction with other materials and/or the environment [1]. This process often occurs in the industry of a material oil and gas. In the industrial field, carbon steel is a type of material that is commonly used for various applications. Carbon steels are used in Algeria and throughout the world for nearly all of the same reasons: their costs, properties, ease of fabrication, availability, weldability, and so on. In most economic sectors and industrial activities carbon steel occupy a preferential position as structural materials. Since they can corrode when exposed to atmospheric, industrial or urban environments with different pollution levels, their practical use always requires specific protection systems against corrosion [2-4] Among these,

*Corresponding author: hammoudanad@yahoo.fr

organic coatings have been of great importance [4-7] As is known, the corrosion protection efficiency of organic coatings depends on a large number of factors, but the adhesion strength at the polymer film/metal substrate interface plays a paramount role [8-10]. The effective life of a coating of anti-corrosive paint applied to a steel surface is to a very large extent dependent on how thoroughly the surface has been prepared prior to painting. One of the most commonly used method for surface preparation is sandblasting used for various purposes of surface influence including: modification [11], strengthening [12], cleaning and rust removal [13]. Sandblasting abrasive particles are smaller compared with particles in shot peening technology. Therefore, a smoother surface can be obtained by sandblasting in general. During the sandblasting process, the surface of samples is blasted repeatedly by sand particles or other hard particles with high speed, which leads to the removal of oxide scale and generation of local plastic deformation in the surface layer. However, Wang et al. [14] observed decrease of corrosion resistance of steel after sandblasting resulting from the existence of high-density lattice defect: dislocation that limits the application possibilities of this technique [15, 16].

2 Experimental Part

2.1 Sample preparation

The metallic substrate was C-1020 carbon steel (according to NF10027 standard) in conformity with the norm API (American Petroleum Industry), used by an Algerian oil company, the chemical composition of the tested steel is given in Table 1. The surface was sandblasted to Sa 1.5 and Sa 2.5 (Swedish Standard SIS 05 59 00/67); Sandblasting was performed by sand particles on a mobile pressure sandblasting machine with a nozzle diameter 6 mm and pressure of 0.6 MPa, removing impurities, millscales, rust and old paint. The microstructure was observed by the light metallographic microscope CARL ZEISS AXIO Imager.A1m (ZEISS, Oberkochen, Germany). 3% Nital was used as an etchant for visualization of the S355J2 steel microstructure. Figure 1a shows the microstructure of tested S355J2 steel and figure 1b shows the surface roughness profile. The microstructure revealed ferrite-pearlite matrix with a low pearlite content (local pearlite occurrence) and with average grain size of 10 μm .

Table1. Chemical composition of C-1020 carbon steel (% in weight)

Component	C	Mn	S	P	Si
wt %	0.16	0.54	0.04	0.04	0.05

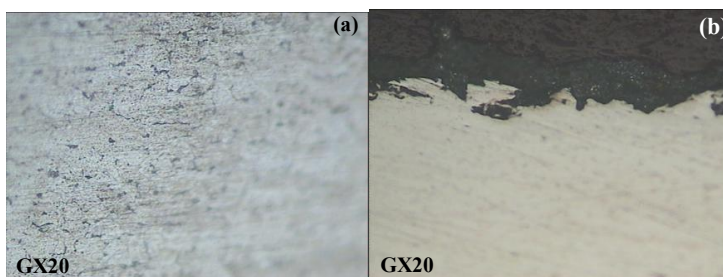


Fig. 1. (a) Microstructure of C-1020 carbon steel. (b) Cross-section images of sandblasted surface.

2.2 Electrochemical Measurements and experimental conditions

Corrosion electrochemical characteristics (corrosion potential) together with kinetic corrosion electrochemical characteristics (corrosion current density and corrosion rate) and

electrochemical impedance spectroscopy corrosion characteristics (polarization resistance) were assessed by corrosion tests in 3% NaCl solution simulating aggressive environment at ambient temperature. The electrochemical measurements were carried out using three-electrode setup comprised of: counter electrode (often a platinum grid or plate), a working electrode of 1cm^2 (the sample under study) and reference electrode (saturated calomel electrode: $\text{Hg}/\text{Hg}_2\text{Cl}_2/\text{KCl sat.}$) was used for electrochemical tests. The potentiodynamic polarization (PD) measurements and electrochemical impedance spectroscopy (EIS) measurements were realized by potentiostat/galvanostat model PGP 201, 230V, 50-60 Hz, at electron configuration connected to a microcomputer allowing potentiostatic polarization measurements to be saved automatically. The time limit for reaching equilibrium potential before doing electrochemical measurement was 30 minutes, frequency range from 100 kHz to 10 MHz [17-19].

3 Results and Discussion

3.1 Influence of degree of sandblasting on the electrochemical behavior of a carbon steel in 3% NaCl solution

3.1.1 Open circuit potential (OCP)

This method consists in following, as a function of time, the evolution of the free potential of corrosion of the sandblasted carbon steel in 3% NaCl medium. The variation of OCP over time for sandblasted carbon steel is shown in Fig.2. To the analysis of Figure 3, we note more electronegative free potential values, they tend towards -0.626 V vs. SCE for the grade Sa 1.5 and towards -0.642 V vs. SCE for the grade Sa 2.5, we find that the value of the potential for the degree of sanding Sa 1.5 is a little higher than that at Sa 2.5, thus presenting a better behavior. This results in continuous degradation of the surface of sandblasted steel, where we find dissolution of the metal.

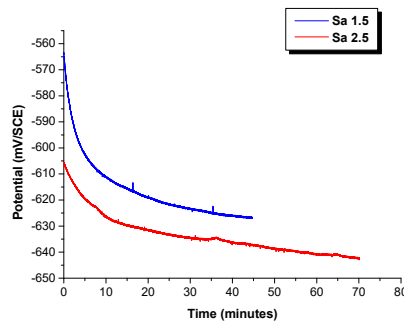


Fig. 2. Variation of OCP with Time of sandblasted carbon steel C-1020 in 3% NaCl solution.

This degradation could be attributed to the roughness of the surface ($40\ \mu$ for the degree Sa 2.5 and $30\ \mu$ for the degree Sa 1.5), because it is a sandblasted steel. So, we are seeing a change in the state of the metal surface where we observe corrosion products. These more or less adherents cause a relative stability of the free potential.

3.1.2 Potentiodynamic polarization curves

Polarization Tafel method was applied to analyze the influence of the degree of sandblasting on the electrochemical behavior of our carbon steel in 3.5% NaCl solution. The electrochemical parameters such as corrosion potential (E_{corr}), current density (i_{corr}), and the polarization resistance (R_p) can be seen from Table 2. Mechanical and chemical surface treatments caused changes in both thermodynamic and kinetic characteristics of the

base material. Thermodynamic stability of the surface is represented by the values of corrosion potentials E_{corr} in our case. More negative value of this electrochemical characteristic means that the surface is less noble and thermodynamically less stable. The kinetics of the corrosion process is directly related to the corrosion current density i_{corr} , when the corrosion current density increases the polarization resistance of our sandblasted carbon steel decreases. This electrochemical characteristic has a direct relation to the corrosion rate r_{corr} [20]; the control governing the kinetics is the charge transfer. From the curves (fig. 3) plotted in 3% NaCl solution, we emphasize a difference between the curve of sandblasted steel at Sa 1.5 and that of steel Sa 2.5. The cathodic curves show in the vicinity of the corrosion potential, a field of diffusion kinetics more marked for Sa 2.5 sandblasted steel only for Sa 1.5 sandblasted steel. The potential at zero current for grade Sa 1.5 is a bit higher than that of grade Sa 2.5, its current density which is of the order of 0.5234 mA/cm² confirms a slow attack of steel contrary to sandblasting Sa 2.5 (0.5330 mA/cm²).

Table 2. The corrosion parameters obtained from polarization plots.

Degree of sandblasting	E_{corr} (mV/ SCE)	i_{cor} (mA/cm ²)	R_p (Ω .cm ²)
Sa 1.5	-811.9	0.5234	77.89
Sa 2.5	-821.2	0.5330	73.80

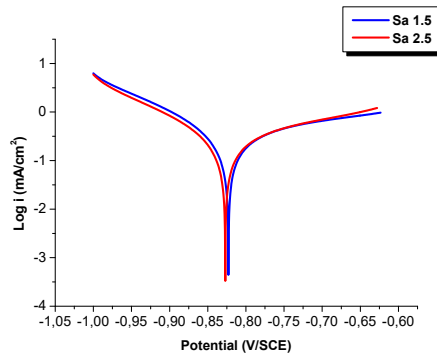


Fig. 3. The representative Tafel polarization plots for sandblasting carbon steel in 3% NaCl solution.

This low current value for the degree Sa 1.5 would be due to the rapid training an oxide film constituting a barrier to the passage of the current with a low R_p value (77.89 Ω .cm²) in relation to the degree Sa 2.5 (73.80 Ω .cm²).

3.2 Transient Electrochemical Methods: Electrochemical Impedance Spectroscopy

3.2.1 Influence of degree of sandblasting on the electrochemical behavior of a carbon steel C-1020 in 3% NaCl solution

The electrochemical impedance diagram obtained for the sandblasted surface at grade Sa 1.5 in 3% NaCl medium under the potential $E_{\text{aban}} = -626$ mV/ ECS and the sandblasted surface at grade Sa 2.5 in the same medium under the potential $E_{\text{aban}} = -642$ mV/ ECS, are shown in Figure 4. The values of various parameters are summarized in Table 3.

Table 3. The parameters obtained from EIS measurements.

Parameters Degree of sandblasting	R_e (Ω .cm ²)	R_{ct} (Ω .cm ²)	C_{dl} (mF/cm ²)
Sa 1.5	12.76	224.1	12.63
Sa 2.5	23.07	212.2	16.79

The impedance diagrams represented in the Nyquist plane (fig.4) show semicircular responses; each of them deviates from the ideal interface because of the presence of heterogeneities, roughness, etc. Since the arcs of the circle are not centered on the real Z axis, for the calculation of the R_{ct} , we extrapolated the "low frequency" part at zero frequency. On the examination of electrochemical impedance diagrams at the free potential of corrosion, a single capacitive loop is observed (a single time constant). The control of electrochemical kinetics is under control of charge transfer.

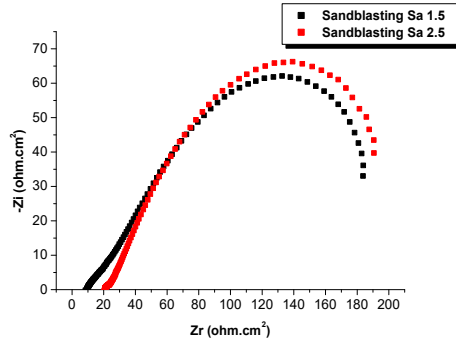


Fig. 4. Evolution of Nyquist diagrams for different degree of sandblasted carbon steel as a function of immersion time in 3% NaCl medium.

The values of the charge transfer resistance R_{ct} determined by extrapolation, shows a slightly high value for grade Sa 1.5 ($224.1 \Omega \cdot \text{cm}^2$) in relation to grade Sa 2.5 ($212.2 \Omega \cdot \text{cm}^2$), thus showing the degradation of the surface of our steel due to sandblasting and the increase of the roughness of the surface with the formation of corrosion products on the metal surface. The values of the capacities which are of the order of $\text{mF} \cdot \text{cm}^2$ are a bit high, $12.63 \text{ mF} \cdot \text{cm}^2$ for state Sa 1.5 and $16.79 \text{ mF} \cdot \text{cm}^2$ for state Sa 2.5, the usual values of double layer capacities are usually of the order of $\mu\text{F} \cdot \text{cm}^2$. This could be attributed to the roughness of the surface following sandblasting and the porous nature of the film corrosion products formed in abandonment and present at the metal interface. The value of the electrolyte resistance R_e is very weak, reflecting the conductivity of the medium. The frequency response of the samples provides information on capacitive behavior affected by the "topography" of the surface, reported by several authors [21, 22]. It consists of the formation of a film of corrosion products adherent and porous thereby increasing the accessible surface.

3.2.2 Equivalent Circuit for the EIS Simulation

The equivalent circuit that reproduces most accurately the impedance diagrams at the metal-electrolyte interface is shown in the figure 5. In this schema, the contribution of the resistance of the electrolyte is simulated by resistance R_{el} , faradic impedance R_{ct} and the double layer capability C_{dl} are parallel. They are characteristic of the metal substrate.

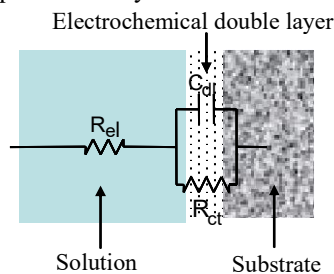


Fig. 5. General equivalent electrical circuit at the electrochemical interface metal-electrolyte.

3.3 Classical electrochemical methods: Influence of immersion time on the electrochemical behavior of the C-1020 carbon steel:

3.3.1 Sandblasted Sa 2.5: Potentiodynamic polarization curves:

We draw the intensity-potential curves around the abandonment potential of the C-1020 carbon steel sanded at grade Sa 2.5 in 3% NaCl solution. The curves of Figure 6 on the behavior of our sanded steel characterize the general appearance of a polarization curve obtained in 3% NaCl medium. Electrochemical parameters like corrosion potential (E_{corr}), corrosion current density (i_{corr}) and polarization resistance (R_p) were determined in Table 4.

Table 4. The corrosion parameters obtained from polarization plots.

Time (hours)	$E_{(i=0)}$ (mV/ ECS)	i_{cor} (mA/cm ²)	R_p (Ω .cm ²)
1	-821	0.53	73.80
6	-815	0.60	65.88
7	-825	0.58	62.53

According to the shape of the curves in Figure 6 and from the analysis of the different electrochemical parameters collected in Table 4 allows us to note a noticeable increase in corrosion current density i_{corr} (0.60 mA/cm²) after six hours immersion in NaCl 3%, thus translating the degradation of our surface condition. The polarization resistance R_p between one hour and seven hours of immersions drops to a value of 62.53 Ω .cm². These results show the role played by the surface state on the polarization resistance, we note for sandblasted carbon steel a low polarization resistance, this is due to sandblasting that cause a macro hardening and differential aeration. Our sandblasted steel will degrade with immersion time following the roughness of the surface; Sandblasting caused a more intensive attack of the steel surface. A destroyed surface with a higher concentration of structure defects and with larger area of an active surface resulted in lower electrochemical stability, which is reflected in the 51 mV decrease of E_{corr} value in comparison with a simply ground surface [23].

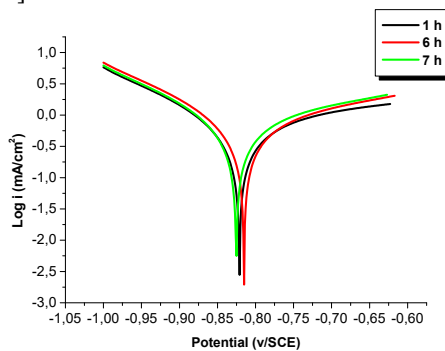


Fig. 6. Influence of the immersion time in 3% NaCl solution on the polarization curves of a sandblasted carbon steel.

3.4. Non-stationary techniques: Electrochemical Impedance Spectroscopy

3.4.1 Influence of immersion time on the electrochemical behavior of the C-1020 carbon steel

The findings from potentiodynamic polarization tests were supported by non-destructive electrochemical impedance spectroscopy (EIS) measurements. Figure 7 shows the Nyquist

diagrams of sandblasted carbon steel samples after different immersion times at free corrosion potential (-642 mV/ECS). Nyquist plots are frequently selected tool for EIS interpretation, allowing precise determination of equivalent circuit components [20, 24, 25].

Electrochemical impedance diagrams, plot for Sa 2.5 sandblasted carbon steel after different immersion times at free corrosion potential (-642 mV/ECS) in Nyquist's plan, are shown in the figure 7, they are characterized by a single capacitive loop. The values of the different parameters are gathered in the table 5. The arcs of the circle are not centered on the real Z axis, for the calculation of the R_p , we extrapolated the "low frequency" part at zero frequency. In 3% NaCl, the values of R_e are very weak, of the order of $20 \Omega \cdot \text{cm}^2$, which shows that our environment is very conducive. To the analysis of impedance diagrams, we notice that from the first hours of immersion a decrease in the charge transfer resistance R_{ct} , the value goes from $212.2 \Omega \cdot \text{cm}^2$ at $100.1 \Omega \cdot \text{cm}^2$ after 21 hours of immersion, the decrease of the R_{ct} could be due to the penetration of the electrolyte as a function of time through the porosity of the corrosion products film, thus promoting the attack of the metal substrate.

This means that the process governing kinetics is under mixed control, charge transfer and diffusion and it is difficult for us to separate the two phenomena. on the other hand the capacity of the double layer C_{dl} we seem very high to be representative of a double layer capacity C_{dl} (of the order of $\text{mF} \cdot \text{cm}^{-2}$) which are usually of the order of $\mu\text{F} \cdot \text{cm}^{-2}$, this could be attributed to the porous nature of the corrosion products present at the metal interface.

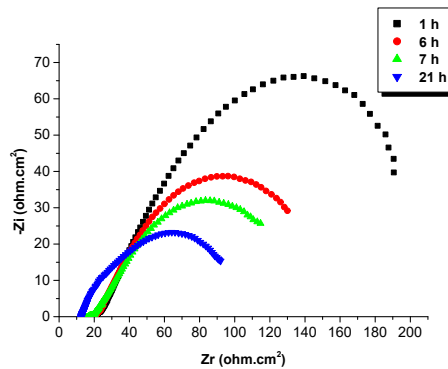


Fig. 7. Evolution of Nyquist plots as a function of immersion time in 3% NaCl solution for sandblasted carbon steel.

Table 5. The parameters obtained from EIS measurements.

Time (hours)	$R_e (\Omega \cdot \text{cm}^2)$	$R_{ct} (\Omega \cdot \text{cm}^2)$	$C_{dc} (\text{mF}/\text{cm}^2)$
1	23.07	212.2	16.79
6	21.64	146.8	27.10
7	20.36	132.5	26.90
21	12.52	100.1	3.17

From the values in the table 5, we notice an increase in double layer capacity after 6 hours of immersion ($27.10 \text{ mF} \cdot \text{cm}^{-2}$) this increase is more or less important (from 16.79 to $27.10 \text{ mF} \cdot \text{cm}^{-2}$) reflecting the degradation of steel, but after 21 hours of immersion it decreases suddenly ($3.17 \text{ mF} \cdot \text{cm}^{-2}$), we think that this decrease in the value of C_{dl} would be due to the formation of corrosion products forming a film more or less adherent on the metal substrate, which plays the role of a barrier. This phenomenon was observed by Duprat and other authors [26, 27], and it has been attributed to the porous nature of the film corrosion products present at the metal interface. The fact that sandblasting deteriorates corrosion properties was observed also on stainless steel [28] as well as pure titanium [29].

3.4.2 Equivalent Circuit for the EIS Simulation

According to figure 5, the control of the electrochemical kinetics is under charge control, the contribution of the resistance of the electrolyte is simulated by R_e , the charge transfer resistance R_{ct} and the double - layer capacitance C_{dl} respectively [30], they are characteristic of the substrate. Charge transfer resistance R_{ct} is the most important electrochemical characteristic. The value of R_{ct} expresses how resistant the mono- or multi- surface layers are against corrosion [31–33].

3.5 Microscopic observation (Optical microscope)

Microscopic observations using the optical microscope of some studied samples were performed before and after test in 3% NaCl medium. Optical microscope observation for sanded state to Sa 2.5 immersed in 3% NaCl solution, highlights the corrosion of our sandblasted carbon steel, following the presence of rust and corrosion products (figure 8).

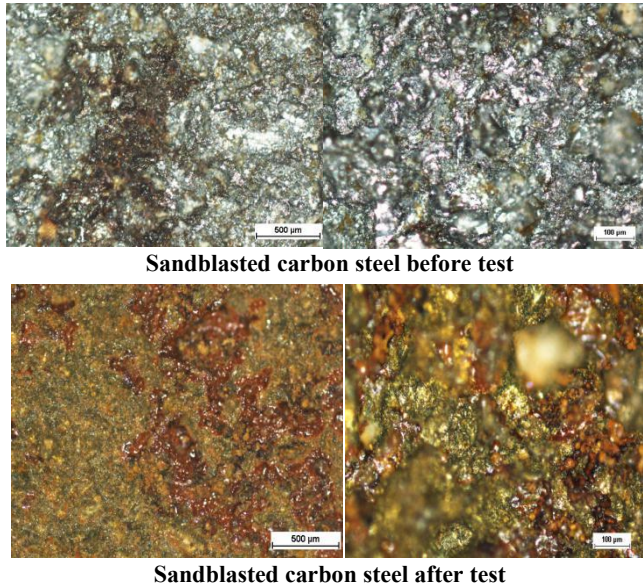


Fig. 8. Micrographs of the different samples.

4 Conclusions

The present work describes the influence of sandblasting surface treatment on morphological and corrosion properties of C-1020 carbon steel. The most relevant conclusion is as follows:

- Sandblasting caused increased surface roughness of the substrate compared to a ground surface.
- Sandblasting had a negative effect on the corrosion resistance of C-1020 carbon steel compared to ground surfaces. Worsening was observed of the relevant electrochemical corrosion characteristics including E_{corr} , i_{corr} , τ_{corr} , and R_p after sandblasting;
- The adhesion grade depends directly on the substrate surface roughness. As the last one increases the number of active sites and consequently the bonding effective surface also increases.
- It must be emphasized that the adhesion strength depends not only on the metal/coating system but also on the surface treatment characteristics.

Acknowledgements

Thanks are due to Sonatrach (Direction Régionale de Skikda, Algeria) for providing sandblasting panels.

References

1. Jones D.A, Principles and Prevention of Corrosion, Macmillan, New York (1992)
2. Rahmel A and W. Scwenk, *Korrosion* 30, 34 (1977).
3. Uhlig H.H and R.W. Revie, *Corrosion and corrosion control* 90, 165-250 (1985).
4. Reinhard G, *Prog. Org. Coatings* 15, 125 (1987).
5. Houwink E.R, *Adhesion and Adhesives* 1, (1965).
6. Zisman W.A, *Adhesion and Cohesion* (1962).
7. Zisman W.A, *Ind. Eng. Chem.* 55, 19 (1963).
8. Wiggle W.A and Smith A.G, *J. Paint Technol.* 40, 174 (1968).
9. Leidheiser Jr.H, *Croat. Chem. Acta* 53, 197 (1980).
10. Walker P, *J. Oil Col. Chem. Assoc.* 65, 415 (1982).
11. Chintapalli R.K, Marro F.G, Jimenez-Pique E, Anglada M. Phase transformation and subsurface damage in 3Y-TZP after sandblasting, *Dent. Mater* 29, 566–572 (2013).
12. Chintapalli R.K, Mestra Rodriguez A, Garcia Marro F, Anglada M. Effect of sandblasting and residual stress on strength of zirconia for restorative dentistry applications, *J. Mech. Behav. Biomed.*29, 126–37 (2014).
13. Raykowski A, Hader M, Maragno B, Spelt J.K. Blast cleaning of gas turbine components: Deposit removal and substrate deformation, *Wear* 249, 126–31 (2001).
14. Wang X.Y, Li D.Y. Mechanical and electrochemical behavior of nanocrystalline surface of 304 stainless steel, *Electrochim. Acta* 47, 3939–47 (2002).
15. Trško L, Bokuvka O, Nový F, Guagliano M. Effect of severe shot peening on ultra-high-cycle fatigue of a low-alloy steel, *Mater. Des.*57, 103–13 (2014).
16. Geng S, Sun J, Guo L. Effect of sandblasting and subsequent acid pickling and passivation on the microstructure and corrosion behavior of 316L stainless steel, *Mater. Design.* 88, 1–7 (2015).
17. Sadeghimeresht E, Markocsan N, Nylén P. A. Comparative Study of Corrosion Resistance for HVOF-Sprayed Fe- and Co-Based Coatings, *Coatings* 6, 16 (2016).
18. Taghavikish M, Subianto S, Dutta N.K, Choudhury N.R. Novel Thiol-Ene Hybrid Coating for Metal Protection, *Coatings* 6, 17 (2016).
19. Pastorek F, Hadzima B, Doležal P. Electrochemical characteristics of Mg-3Al-1Zn alloy surface with hydroxyapatite coating, *Communications* 14, 26–30 (2012).
20. Hadzima B, Mhaede M, Pastorek F. Electrochemical characteristics of calcium-phosphatized AZ31 Magnesium alloy in 0.9% NaCl Solution, *J. Mat. Sci. Mat. Med.*25, 1227–37 (2014).
21. Bonnel A, Dabosi F, Delouis C, Duprat M, Keddami M, Tribollet B, *J. Electrochem. Soc.*130, 753 (1983).
22. Dabosi F, Delouis C, Duprat M, Keddami M, *J. Electrochem.Soc.Electrochem.Sciences and Technology*, 761 (1983).

23. Pastorek F, Borko K, Fintová S, Kajánek D, Hadzima B. Effect of Surface Pretreatment on Quality and Electrochemical Corrosion Properties of Manganese Phosphate on S355J2 HSLA Steel, *Coatings* 6, 46 (2016).
24. Tokash Wei, Zhang B, J.C. Kim F, Logan Y, B.E. Electrochemical analysis of separators used in single-chamber, air–cathode microbial fuel cells, *Electrochim. Acta* 89, 45–51 (2013).
25. Han X.G, Zhu F, Zhu X.P, Lei M.K, Xu J.J. Electrochemical corrosion behavior of modified MAO film on magnesium alloy AZ31 irradiated by high-intensity pulsed ion beam, *Surf. Coat. Technol.* 228, 164–70 (2013).
26. Breur H. J. A , Ferrari G. M , van Turnhout J, de Wit J. H. W Modern experimental techniques for the assessment of the water sensitivity of organic coatings, *Symposium New trends in organic coatings for marine environments*, Lisbon, 22-24 July (1998).
27. Hammouda N, Chadli H, Guillemot G, Belmokre K. The Corrosion Protection Behaviour of Zinc Rich Epoxy Paint in 3% NaCl Solution, *Adv. Chem. Eng. Sci.* 01, 51–60 (2011).
28. Geng S, Sun J, Guo L. Effect of sandblasting and subsequent acid pickling and passivation on the microstructure and corrosion behavior of 316L stainless steel, *Mater. Design.* 88, 1–7 (2015).
29. Jiang X.P, Wang X.Y, Li J.X, Li D.Y, Man C.-S, Shepard M.J, Zhai T. Enhancement of fatigue and corrosion properties of pure Ti by sandblasting, *Mater. Sci. Eng. A* 429, 30–35 (2006).
30. Azzouz N. These, *LCTS, univ. Franche-compte*, France (1992).
31. Mhaede M, Pastorek F, Hadzima B. Influence of shot peening on corrosion properties of biocompatible magnesium alloy AZ31 coated by dicalcium phosphate dihydrate (DCPD), *Mater. Sci. Eng.* 39, 330–35 (2014).
32. Frankel G.S. Electrochemical techniques in corrosion: Status, limitations, and needs, *J. ASTM Int.* 5, 30–40 (2008).
33. Ariza E, Rocha L.A. Evaluation of corrosion resistance of multi-layered Ti/glass–ceramic interfaces by electrochemical impedance spectroscopy, *Mater. Sci. Forum.* 492, 189–94 (2005).